SOLID-STATE PHYSICS

Signatures of exciton condensation in a transition metal dichalcogenide

Anshul Kogar,[1] Melinda S. Rak,[1] Sean Vig,[1] Ali A. Husain,[1] Felix Flicker,[2] Young Il Joe,[1] Luc Venema,[1]* Greg J. MacDougall,[1] Tai C. Chiang,[1] Eduardo Fradkin,[1] Jasper van Wezel,[3] Peter Abbamonte[1]†

Bose condensation has shaped our understanding of macroscopic quantum phenomena, having been realized in superconductors, atomic gases, and liquid helium. Excitons are bosons that have been predicted to condense into either a superfluid or an insulating electronic crystal. Using the recently developed technique of momentum-resolved electron energy-loss spectroscopy (M-EELS), we studied electronic collective modes in the transition metal dichalcogenide semimetal 1*T*-$TiSe_2$. Near the phase-transition temperature (190 kelvin), the energy of the electronic mode fell to zero at nonzero momentum, indicating dynamical slowing of plasma fluctuations and crystallization of the valence electrons into an exciton condensate. Our study provides compelling evidence for exciton condensation in a three-dimensional solid and establishes M-EELS as a versatile technique sensitive to valence band excitations in quantum materials.

If a fluid of bosons is cooled to sufficiently low temperature, a substantial fraction will condense into the lowest quantum state, forming a Bose condensate. Bose condensation is a consequence of the even symmetry of the many-body wave function of bosons under particle interchange and allows for the manifestation of macroscopic quantum phenomena, the most notable of which is superfluidity.

Traditionally, Bose condensates are said to exist in two types: Bose-Einstein condensates (BECs) occur in systems of stable bosons, such as dilute atomic gases or liquid ^{4}He, whereas in Bardeen-Cooper-Schrieffer (BCS) condensates the bosons are formed of bound states of fermions, such as the Cooper pairs in a superconductor or superfluid ^{3}He. In reality, all such bosons (e.g., a ^{4}He atom) are composed of bound fermions, and BECs and BCS condensates are just different limits of the same phase of matter (*1*). Experiments on such condensates have shaped the modern understanding of quantum field theory (*1*).

Excitons are bosons that are bound states between an electron and hole in a solid and were predicted long ago to Bose condense (*2*–*4*). Because of their light mass and high binding energy, exciton condensates should be stable at higher temperature than for traditional BEC or BCS phases (*5*, *6*). Different theories predict that a Bose condensate of excitons could be a superfluid (*5*) or innately insulating (*7*), so there is tremendous need for experimental input. Identifying an exciton condensate in nature could have a profound effect on future understanding of macroscopic quantum phenomena, as well the classic problem of the metal-insulator transition in band solids, in which exciton condensation has long been believed to play a fundamental role (*2*–*4*).

Condensed phases of photogenerated excitons have been realized in semiconductor quantum wells in resonance with a Fabry-Perot cavity. These systems, although not fully thermally equilibrated, have exhibited evidence for transient superfluidity (*8*). Excitonic phases have also been realized in quantum Hall bilayers in a perpendicular magnetic field (*9*). Although the order in these two-dimensional (2D) structures is not strictly long ranged and the order parameter cannot be measured directly, compelling evidence for excitonic correlations has been observed in Coulomb drag experiments (*9*). Despite these achievements, there is a great need to identify an exciton condensate in a fully thermalized 3D system in which the order is long ranged.

An ideal approach would be to identify a material in which an exciton condensate forms naturally. Long ago, a BCS condensate of excitons was predicted to arise spontaneously in semimetals in which an indirect band gap is tuned close to zero (Fig. 1) (*2*–*4*). This condensate is expected to break a spatial symmetry, rather than the *U*(1) symmetry broken by a superconductor, and in the absence of pinning should exhibit perfect conductivity without a Meissner effect (*10*). This phase can be thought of as a solid crystal of excitons, which Halperin and Rice dubbed "excitonium" (*4*), and is the two-band analog of the Wigner crystal instability of an interacting electron gas (*10*). This condensate is closely related to that in bilayer quantum wells (*9*), although the coherence develops between electrons and holes in different bands (Fig. 1) rather than in different layers. If detected, this exciton condensate would be 3D, guaranteed to reside in thermodynamic equilibrium, and could potentially be stable close to room temperature, facilitating fundamental studies of this many-body phenomenon (*2*–*4*, *7*).

The challenge is that an exciton condensate in a solid is nearly impossible to distinguish from a Peierls charge density wave. A Peierls phase is a spontaneous crystal distortion driven by the electron-phonon interaction (*11*) and is unrelated to exciton formation. However, the two phases have the same symmetry and similar physical observables, such as the existence of a superlattice and the opening of a single-particle energy gap. Although many compelling candidate excitonic materials have been identified (*12*–*17*), an experimental means to distinguish between

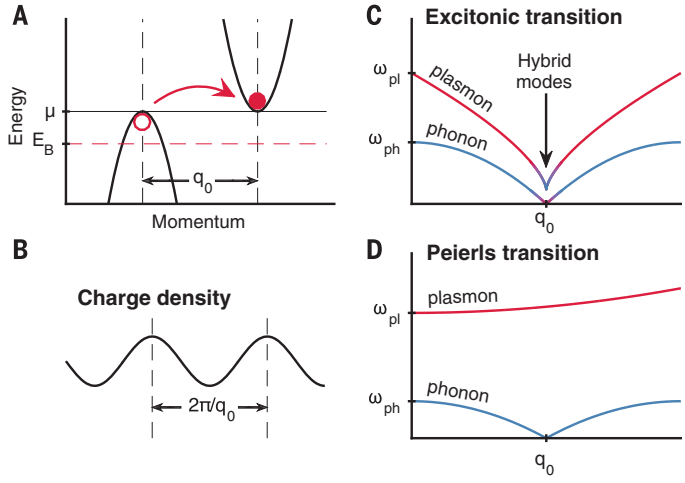

Fig. 1. Collective excitations of a material containing a condensate of excitons. (**A**) Excitons spontaneously condense when electrons and holes bind between two bands whose extrema lie near the chemical potential, separated by wave vector q_0. E_B, exciton binding energy; μ, chemical potential. (**B**) Exciton condensation leads to a modulation in the charge density with period $2\pi/q_0$. (**C**) Sketch of the collective excitations of an exciton condensate in a solid with lattice degrees of freedom. Both electronic and lattice modes soften at the phase-transition temperature (T_C). At q_0, hybrid modes are formed, only one of which reaches zero energy. ω_{pl}, plasma frequency; ω_{ph}, phonon frequency. (**D**) Sketch of the excitations of a conventional Peierls charge density wave, in which the only soft mode is a phonon.

[1]Department of Physics and Seitz Materials Research Laboratory, University of Illinois, Urbana, IL 61801, USA. [2]Rudolph Peierls Centre for Theoretical Physics, University of Oxford, Oxford OX1 3NP, UK. [3]Institute of Physics, University of Amsterdam, 1098 XH Amsterdam, Netherlands.
*Deceased.
†Corresponding author. Email: abbamonte@mrl.illinois.edu

Peierls and excitonic ground states (that is, to determine whether an electron-hole condensate is present) has been lacking.

We demonstrate the existence of an exciton condensate in 1*T*-$TiSe_2$ by using momentum-resolved electron energy-loss spectroscopy (M-EELS) to measure its collective excitations (*18*). The defining characteristic of a Peierls phase is the presence of a soft phonon whose energy falls to zero at finite momentum, q_0, at its phase-transition temperature [critical temperature (T_C)] (*11*, *19*). Below T_C, this phonon splits into amplitude and phase branches, the latter (if it remains gapless) serving as the Goldstone mode (*11*, *19*).

In contrast, the Goldstone mode of an exciton condensate corresponds to translation of the electronic crystal with respect to the atomic lattice and was dubbed "excitonic sound" by Kohn (*20*). The precursor to this mode at $T > T_C$ is an electronic, plasmon-like excitation, which defines the excitonic transition by falling to zero energy at T_C. This electronic mode can mix with phonons at low energy but should disperse to the plasma frequency as $q \rightarrow 0$ (*20*). In other words, a material could be established to contain an exciton condensate if it exhibited a soft plasmon, analogous to the soft phonon of a Peierls transition (*4*, *17*, *20*).

The observation of an electronic mode that falls to zero energy at finite momentum would indicate that the energy to create an electron-hole pair is zero, which is unambiguous evidence for condensation of electron-hole pairs (that is, the development of a macroscopic population of excitons in the ground state). Hereafter, we will refer to this electronic mode as a plasmon, although elucidating its exact character—including whether it is longitudinal, transverse, or a mixture of the two—requires further theoretical and experimental study.

One of the most promising candidate excitonic materials is the transition metal dichalcogenide semimetal 1*T*-$TiSe_2$, whose vanishing indirect band gap is optimal for realizing an exciton condensate (*2*–*4*, *17*). At T_C = 190 K, $TiSe_2$ exhibits a resistive anomaly and forms a $2a \times 2a \times 2c$ superlattice (where a and c are lattice parameters) whose wave vector connects the Se 4p valence band at the Γ point to the Ti 3d conduction band at the L point, leading many authors to identify the material as residing in an excitonic state (*17*, *21*, *22*). However, $TiSe_2$ also exhibits a sizeable lattice distortion (*17*, *23*), prompting others to argue that it is a phonon-driven Peierls-like phase (*24*–*28*).

M-EELS studies of $TiSe_2$ were carried out at a beam energy of 50 eV, using an Ibach-type high-resolution EELS spectrometer (*29*). Momentum resolution was achieved by precisely aligning the spectrometer to the rotation axes of a low-temperature sample goniometer operated with a custom control system adapted from x-ray diffraction (*18*). M-EELS measures the charge dynamic structure factor of a surface, $S(\mathbf{q}, \omega)$, which is proportional to the imaginary part of the frequency- and momentum-dependent charge susceptibility, $\chi''(\mathbf{q}, \omega)$ (*18*). This quantity is proportional to the dielectric loss function, $-\mathrm{Im}[1/\varepsilon(\mathbf{q}, \omega)]$ (*30*), so M-EELS can be thought of as momentum-resolved infrared (IR) spectroscopy. M-EELS is more sensitive to valence band excitations than inelastic x-ray or neutron scattering, which mainly couple to lattice modes, and is particularly suited to studies of electronic collective excitations (*18*). The results presented here were replicated five times on different cleaved crystals, each of which provided reproducible data for ~40 hours under ultrahigh vacuum conditions (fig. S6) (*31*).

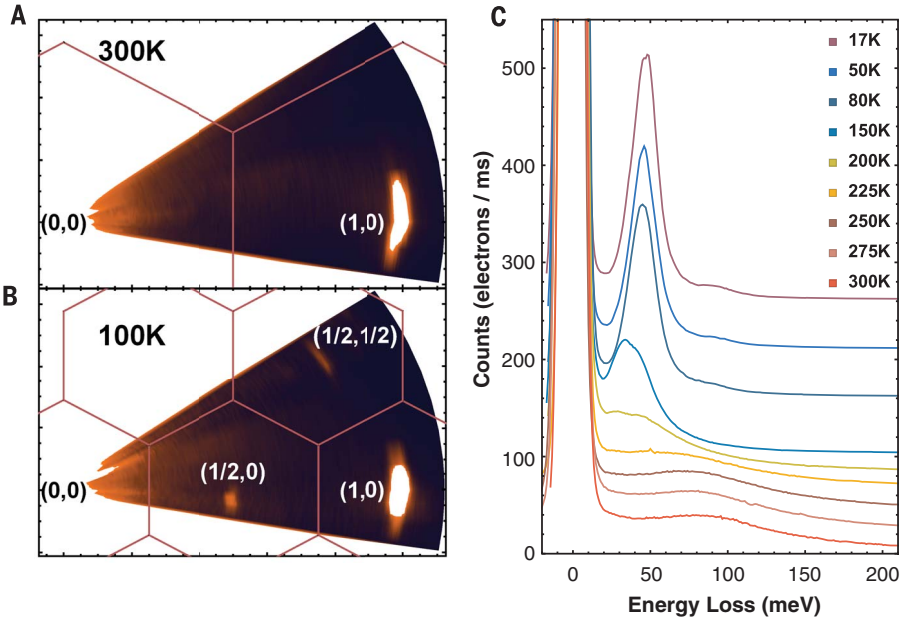

Fig. 2. Consistency between M-EELS data and previous studies of $TiSe_2$. (**A**) Elastic ($\omega = 0$) momentum map of $TiSe_2$ at room temperature, showing the Brillouin zone boundaries (light brown lines) and the (1, 0) Bragg peak. (**B**) Same map as in (A), showing the appearance, at $T < T_C$, of superlattice reflections at (0.5, 0) and (0.5, 0.5), consistent with previous x-ray and neutron scattering studies (*17*, *23*, *36*). These reflections denote the development of a macroscopic population of excitons. (**C**) M-EELS spectra at $\mathbf{q} = 0$, showing an electronic mode at 82 meV that shifts and sharpens below T_C (spectra have been offset vertically for clarity), in quantitative agreement with previous studies using IR spectroscopy (*32*–*34*).

M-EELS measurements of $TiSe_2$ are consistent with experimental results obtained with other methods. Figure 2, A and B, shows static (frequency $\omega = 0$) M-EELS maps of momentum space taken with an energy resolution of 6 meV. Superlattice reflections, indicating the breaking of translational symmetry and the development of a static order parameter, appear below T_C at wave vectors $\mathbf{q}$ = (0.5, 0) and (0.5, 0.5) (because M-EELS is a surface probe, momenta are indexed using only the two components parallel to the surface). The peak locations are in quantitative agreement with x-ray, neutron, and electron diffraction studies (*17*, *23*).

Frequency-dependent M-EELS spectra, taken at a fixed momentum $\mathbf{q} = 0$ for a series of temperatures, are shown in Fig. 2C. At T = 300 K, a highly damped electronic mode, the energy and linewidth of which decrease when cooling through T_C, is observed at 82 meV. The mode energy increases again at low temperature, reaching 47 meV at T = 17 K. These changes agree quantitatively with previous IR spectroscopy studies (*32*–*34*), which identified this excitation as a free-carrier plasmon because its energy is substantially higher than that of the highest optical phonon at 36 meV (*27*, *35*). These changes in plasmon energy and linewidth were interpreted as a decrease in carrier density and Landau damping caused by opening an energy gap at T_C (*32*–*34*).

The plasmon in Fig. 2C is the fundamental electronic collective mode of $TiSe_2$. The question of whether an exciton condensate is present can be simplified to asking whether this excitation exhibits the behavior of a soft mode at T_C.

At $T > T_C$ (Fig. 3A), the momentum dependence of the plasmon in $TiSe_2$ is unremarkable. Its energy and linewidth increase along the (1, 0) direction with increasing $\mathbf{q}$, consistent with the usual Lindhard description of a conductor (*30*). Upon cooling to T = 185 K ~ T_C (Fig. 3B), the plasmon becomes anomalous: its energy decreases with increasing $\mathbf{q}$ until it merges with the zero-loss line for $\mathbf{q} > (0.3, 0)$. Near the ordering wave vector, $\mathbf{q_0} = (0.5, 0)$, the excitation is gapless within the resolution of the measurement, and the M-EELS spectrum exhibits a power law form, $S \sim \omega^{-1}$ (*31*). At momenta $\mathbf{q} > (0.7, 0)$, the electronic mode emerges again, increasing in energy to its maximum value at $\mathbf{q}$ = (1, 0). This behavior is exactly what is expected of a soft mode (*11*, *19*).

Upon cooling further to T = 100 K (Fig. 3C), well below T_C, the excitation hardens, forming

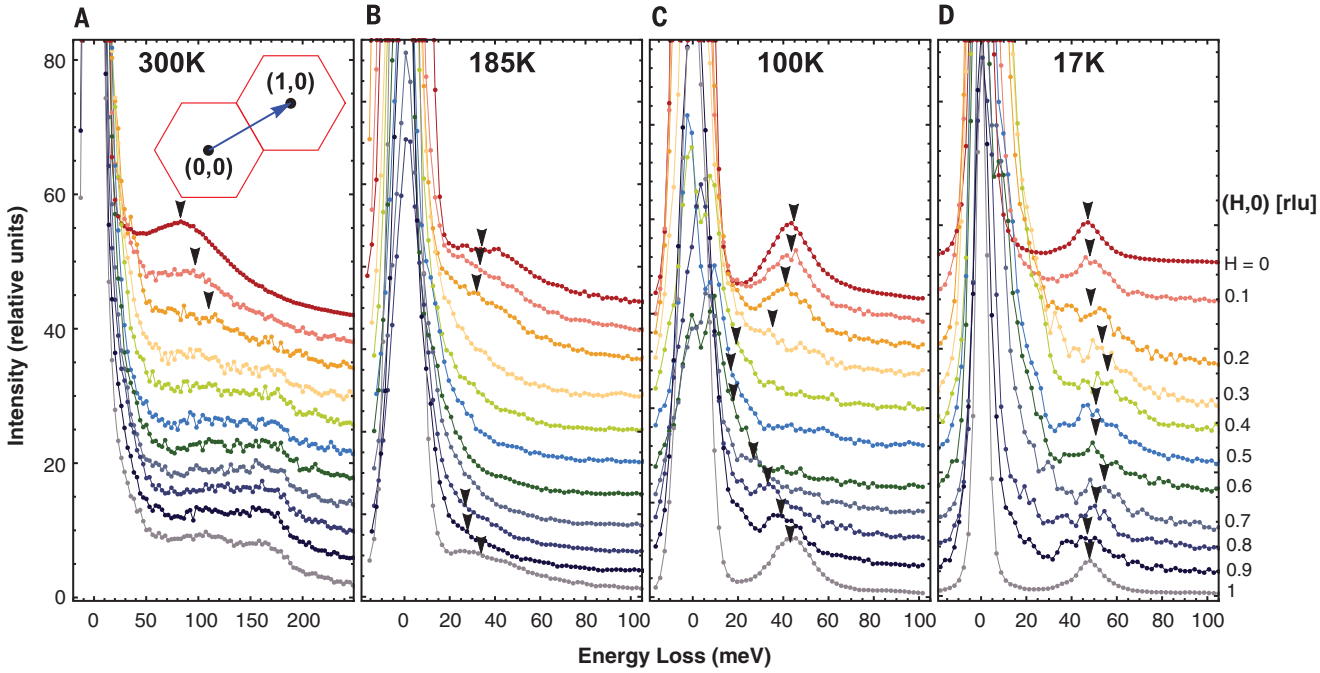

Fig. 3. Momentum dependence of the valence plasmon in $TiSe_2$ for different temperatures. (**A**) Normal-state M-EELS spectra, showing a plasmon at ω = 82 meV that exhibits conventional, Lindhard-like dispersion (*30*). (**B**) Spectra near T_C, where electronic and lattice excitations cease to be resolvable. The electronic mode at this temperature reverses its dispersion, going soft at **q** = (0.5, 0). (**C**) Spectra at T = 100 K, showing hardening of the electronic mode. (**D**) Spectra at T = 17 K, showing a fully hardened, nondispersive electronic mode at ω = 47 meV. Arrowheads indicate the peak energy determined from our data fit (*31*). H, Miller index; rlu, reciprocal lattice units.

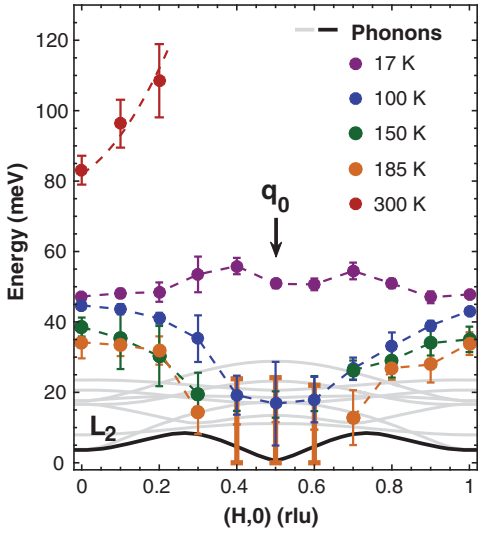

Fig. 4. Summary of the momentum dependence of the soft plasmon mode in $TiSe_2$. Dispersion curves along the (1, 0) momentum direction were determined by fitting the raw spectra in Fig. 3 (*31*). The error bars represent statistical and systematic contributions, the latter determined by applying several different fit models to the data (*31*). Thick, vertical bars denote spectra that exhibit a power law form, $S \sim \omega^{-1}$, instead of a discernable peak. For comparison, the solid lines show the phonon dispersions along the $A \rightarrow L$ direction at $T = T_C$ [reproduced from (*41*)]. Only the L_2 mode (black line) participates in the phase transition. The plasmon behavior is that of the soft mode of a phase transition (Fig. 1C), demonstrating the condensation of electron-hole pairs at T_C.

a dispersing mode that is resolvable at $\mathbf{q_0}$ = (0.5, 0) as a shoulder on the elastic line. By T = 17 K (Fig. 3D), the mode hardens to 47 meV, and its energy and linewidth become approximately momentum independent.

This unusual plasmon mode was not observed in inelastic x-ray (*36*) and neutron (*35*) scattering experiments, which lack the valence sensitivity of M-EELS (*18*). We quantified its behavior by fitting the spectra with a series of Gaussian and Lorentzian functions for the elastic peak, several phonons, and the plasmon mode, including both Stokes and anti-Stokes (energy gain) features (Fig. 4) (*31*).

The behavior displayed in Fig. 4 is that of a soft mode, demonstrating that electron-hole pairs in $TiSe_2$ are condensing at T_C, forming a Bose condensate of excitons. The overall picture that emerges is that, at $T > T_C$, $TiSe_2$ is an ordinary semimetal with a free-carrier plasmon at plasma frequency ω_p = 82 meV. As the system is cooled toward T_C, the plasma fluctuations slow down, particularly at $\mathbf{q} = \mathbf{q_0}$. The electron spectral function, as measured by angle-resolved photoemission spectroscopy (ARPES), begins to show the precursor to an energy gap (*17*, *22*, *25*, *37*), and the plasmon shifts to lower frequency and becomes overdamped (Fig. 3 and 4). Slightly above T_C, the correlation function, $S(\mathbf{q_0},\omega)$, exhibits power laws indicating dynamical critical fluctuations (*31*). At $T = T_C$, a single-particle gap opens, the mean plasmon energy reaches zero, and a finite population of excitons forms, leading to a static (ω = 0), resolution-limited order parameter reflection at $\mathbf{q_0}$ (Fig. 2B). Below T_C, the population of the condensate becomes macroscopic, a spectral gap in ARPES is established, and the plasmon hardens into an amplitude mode that is only weakly dispersive (Fig. 4). This excitation, identified as a plasmon in IR studies (*32*–*34*), is better thought of as an exciton because it represents a quantized modulation of the amplitude of the condensate. To what extent this excitation exhibits the character of a conventional plasmon as $\mathbf{q} \rightarrow 0$ remains an open question. The associated phase mode was not observed in M-EELS and may not exist as a distinct excitation in a condensate with period $2a$ because its order parameter is real. A microscopic model is needed to know for certain.

The lattice degrees of freedom are not inert in $TiSe_2$, which exhibits a sizeable lattice distortion (*17*, *23*), implying the existence of a soft phonon. As illustrated in Fig. 4, only one of the nine phonon branches in $TiSe_2$—the transverse L_2 mode, which goes soft at T_C—participates in the phase transition (*35*, *36*). The L_2 distortion may be a passive consequence of the excitonic

state. However, several authors have suggested that, if an exciton condensate is present, this transverse lattice distortion may help stabilize it (*37*, *38*). In this situation, the L_2 phonon and soft plasmon must interact.

Although experiments lack the resolution to determine for certain, we speculate that the plasmon and L_2 phonon interact as sketched in Fig. 1C. At $\mathbf{q} = 0$, the two excitations should be distinct. If both contribute to the transition, at $T = T_C$ both will soften toward zero energy at $\mathbf{q} = \mathbf{q_0}$. The electron-phonon interaction will cause the two modes to mix, leading to an avoided crossing near $\mathbf{q_0}$ where the hybrid excitations have equal phonon and plasmon character. Only one will act as a soft mode, the other remaining at finite energy. Note that this mixing should only be nonzero if the electronic mode itself also exhibits some transverse character, though additional studies are required to ascertain this. The condensed electron-hole pairs are then dressed by phonons, creating a lattice distortion that coexists with the exciton condensate.

Nevertheless, $TiSe_2$ is qualitatively different from Peierls materials, which behave as illustrated in Fig. 1D. The only soft mode in a Peierls transition is a phonon, as the plasmon exhibits no change near T_C. Examples of Peierls materials are $NbSe_2$ and TaS_2, in which strong metallic screening prevents excitons from forming, and the plasmon resides at high energy ($\omega_p \sim 1$ eV) and is unaffected by the phase transition (*39*). Weak mixing between plasmon and phonon modes still occurs because the electron-phonon interaction is nonzero. But the degree of mixing is on the order of g/ω_p, where g is a plasmon-phonon coupling constant. Using the theory described in (*40*), we estimate $g \sim 6$ meV in $NbSe_2$, implying $g/\omega_p \sim 0.006$, which means that the soft mode is less than 1% electronic in character, compared with ~50% for the case of an excitonic state. Hence, the distinction between an exciton condensate and a Peierls phase is, ultimately, a quantitative matter. $TiSe_2$ is distinct in that the electronic character of its ordered state is orders of magnitude larger than any other material, setting it apart as hosting a crystalline state of solid excitonic matter.

REFERENCES AND NOTES

1. A. J. Leggett, *Science* **319**, 1203–1205 (2008).
2. N. F. Mott, *Philos. Mag.* **6**, 287–309 (1961).
3. L. V. Keldysh, Y. V. Kopaev, *Sov. Phys. Solid State* **6**, 2219–2224 (1965).
4. B. I. Halperin, T. M. Rice, *Rev. Mod. Phys.* **40**, 755–766 (1968).
5. D. Snoke, *Science* **298**, 1368–1372 (2002).
6. M. S. Fuhrer, A. R. Hamilton, *Physics* **9**, 80 (2016).
7. W. Kohn, D. Sherrington, *Rev. Mod. Phys.* **42**, 1–11 (1970).
8. A. Amo *et al*., *Nat. Phys.* **5**, 805–810 (2009).
9. J. P. Eisenstein, *Annu. Rev. Condens. Matter Phys.* **5**, 159–181 (2014).
10. A. J. Beekman, J. Nissinen, K. Wu, J. Zaanen, *Phys. Rev. B* **96**, 165115 (2017).
11. G. Grüner, *Density Waves in Solids* (Perseus, 1994).
12. J. Neuenschwander, P. Wachter, *Phys. Rev. B* **41**, 12693–12709 (1990).
13. Y. Wakisaka *et al*., *Phys. Rev. Lett.* **103**, 026402 (2009).
14. V. N. Kotov, B. Uchoa, V. M. Pereira, F. Guinea, A. H. Castro Neto, *Rev. Mod. Phys.* **84**, 1067–1125 (2012).
15. E. Tosatti, P. W. Anderson, *Solid State Commun.* **14**, 773–777 (1974).
16. D. E. Logan, P. P. Edwards, *Ber. Bunsenges. Phys. Chem* **90**, 575–581 (1986).
17. K. Rossnagel, *J. Phys. Condens. Matter* **23**, 213001 (2011).
18. S. Vig *et al*., *SciPost Phys.* **3**, 026 (2017).
19. J. P. Pouget, B. Hennion, C. Escribe-Filippini, M. Sato, *Phys. Rev. B* **43**, 8421–8430 (1991).
20. W. Kohn, in *Many Body Physics*, C. Dewitt, L. Balian, Eds. (Gordon and Breach, 1968), pp. 355–395.
21. J. A. Wilson, *Solid State Commun.* **22**, 551–553 (1977).
22. H. Cercellier *et al*., *Phys. Rev. Lett.* **99**, 146403 (2007).
23. F. J. Di Salvo, D. E. Moncton, J. V. Waszczak, *Phys. Rev. B* **14**, 4321–4328 (1976).
24. N. Suzuki, A. Yamamoto, K. Motizuki, *J. Phys. Soc. Jpn.* **54**, 4668–4679 (1985).
25. T. E. Kidd, T. Miller, M. Y. Chou, T. C. Chiang, *Phys. Rev. Lett.* **88**, 226402 (2002).
26. K. Rossnagel, L. Kipp, M. Skibowski, *Phys. Rev. B* **65**, 235101 (2002).
27. M. Calandra, F. Mauri, *Phys. Rev. Lett.* **106**, 196406 (2011).
28. H. P. Hughes, *J. Phys. C* **10**, L319–L323 (1977).
29. H. Ibach, D. L. Mills, *Electron Energy Loss Spectroscopy and Surface Vibrations* (Academic Press, 1982).
30. D. Pines, P. Nozieres, *Theory of Quantum Liquids* (Perseus, 1999).
31. Materials and methods are available as supplementary materials.
32. J. A. Wilson, A. S. Barker Jr., F. J. DiSalvo Jr., J. A. Ditzenberger, *Phys. Rev. B* **18**, 2866–2875 (1978).
33. W. Y. Liang, G. Lucovsky, J. C. Mikkelsen, R. H. Friend, *Philos. Mag. B* **39**, 133–146 (1979).
34. G. Li *et al*., *Phys. Rev. Lett.* **99**, 027404 (2007).
35. N. Wakabayashi, H. G. Smith, K. C. Woo, F. C. Brown, *Solid State Commun.* **28**, 923–926 (1978).
36. F. Weber *et al*., *Phys. Rev. Lett.* **107**, 266401 (2011).
37. C. Monney, G. Monney, P. Aebi, H. Beck, *New J. Phys.* **14**, 075026 (2012).
38. J. van Wezel, P. Nahai-Williamson, S. S. Saxena, *Phys. Rev. B* **81**, 165109 (2010).
39. J. van Wezel *et al*., *Phys. Rev. Lett.* **107**, 176404 (2011).
40. F. Flicker, J. van Wezel, *Nat. Commun.* **6**, 7034 (2015).
41. M. Holt, P. Zschack, H. Hong, M. Y. Chou, T.-C. Chiang, *Phys. Rev. Lett.* **86**, 3799–3802 (2001).

ACKNOWLEDGMENTS

We thank C. M. Varma, A. H. MacDonald, G. Baym, and A. J. Leggett for discussions and I. Bozovic, J. D. Stack, and S. A. Kivelson for feedback on the manuscript. This work was funded by the Gordon and Betty Moore Foundation's EPiQS Initiative through grant GBMF-4542. Development of the M-EELS instrument was supported by the U.S. Department of Energy (DOE) Center for Emergent Superconductivity, an Energy Frontier Research Center funded by the DOE Office of Science under award DE-AC02-98CH10886, with equipment provided by DOE grants DE-FG02-08ER46549 and DE-FG02-07ER46453. J.v.W. acknowledges support from a VIDI grant from the Netherlands Organization for Scientific Research (NWO). G.J.M. and E.F. acknowledge support from DOE grant DE-SC0012368. T.C.C. acknowledges support from DOE grant DE-FG02-07ER46383. F.F. acknowledges support from a Lindemann Trust Fellowship of the English Speaking Union and the Astor Junior Research Fellowship of New College, University of Oxford. The data presented in this manuscript are available from the authors upon reasonable request.

SUPPLEMENTARY MATERIALS

www.sciencemag.org/content/358/6368/1314/suppl/DC1
Materials and Methods
Supplementary Text
Figs. S1 to S6

23 December 2016; accepted 24 October 2017
10.1126/science.aam6432

Signatures of exciton condensation in a transition metal dichalcogenide

Anshul Kogar, Melinda S. Rak, Sean Vig, Ali A. Husain, Felix Flicker, Young Il Joe, Luc Venema, Greg J. MacDougall, Tai C. Chiang, Eduardo Fradkin, Jasper van Wezel and Peter Abbamonte

Science **358** (6368), 1314-1317.
DOI: 10.1126/science.aam6432

Probing an excitonic condensate

Excitons—bound states of electrons and holes in solids—are expected to form a Bose condensate at sufficiently low temperatures. Excitonic condensation has been studied in systems such as quantum Hall bilayers where physical separation between electrons and holes enables a longer lifetime for their bound states. Kogar *et al.* observed excitons condensing in the three-dimensional semimetal 1 *T*-$TiSe_2$. In such systems, distinguishing exciton condensation from other types of order is tricky. To do so, the authors used momentum-resolved electron energy-loss spectroscopy, a technique developed to probe electronic collective excitations. The energy needed to excite an electronic mode became negligible at a finite momentum, signifying the formation of a condensate.

Science, this issue p. 1314